THE USE OF SPATIAL CONSTRAINTS IN THE DERIVATION OF MESOSCALE SEA SURFACE CURRENT FIELDS FROM MULTI-SENSOR SATELLITE DATA

Benjamin Seppke[1], Martin Gade[2], and Leonie Dreschler-Fischer[1]

[1]University of Hamburg, Dept. of Informatics, Cognitive Systems Laboratory, Hamburg, Germany
[2]University of Hamburg, Centre for Marine and Atmospheric Sciences, Institute of Oceanography, Hamburg, Germany

ABSTRACT

Sequential multi-sensor satellite images are used for the computation of mesoscale surface currents in the Northern and Southern Baltic Proper. Different marine surface films and accumulated algae at the water surface are imaged by the sensors working in the optical, infrared, and microwave part of the electromagnetic spectrum and can thus be used as tracers for the local motion of the sea surface. Due to the generality of the problem, there are different algorithms available for motion estimation using object tracking in images. To apply these to the field of sea surface current estimation, we need to take the smoothness assumptions into account that the algorithms were built up on. We present the influence of different spatial constraints in the algorithms for the derivation of mesoscale sea surface currents using multi-sensor / multi-channel satellite images by means of a quantitative comparison with model results provided by the German Federal and Maritime Agency (BSH).

Index Terms— oceanography, sea surface currents, motion estimation, multi-sensor

1. INTRODUCTION

Mesoscale dynamic sea surface features, such as eddies, fronts, or dipoles, are of key importance for our understanding of local dynamics of the marine coastal environment. However, they are often not fully resolved by numerical models currently in use. Series of satellite images (with resolutions ranging from a few meters to hundreds of meters), acquired within a short time period (from less than an hour to a day), can be used to close this gap, if the spatial and temporal extent of those dynamic surface features fits to the spatial and temporal resolution of the sensors and of the data acquisitions, respectively. Moreover, current tracers that are detectable by all applied sensors, need to be present during the whole time of image acquisitions.

In this paper, we present the use of spatial constraints in algorithms for the derivation of mesoscale sea surface currents using multi-sensor / multi-channel satellite images. In order to show example results of the methods we have selected satellite data from different sensors imaging the Baltic Sea. We will compare our results quantitatively with the sea surface currents that have been predicted from the German Federal and Maritime Agency (BSH) [6] instead of comparing them directly with each other.

2. SATELLITE DATA

The images were acquired by the Thematic Mapper (TM), the ERS-2 Synthetic Aperture Radar (SAR) and the Sea Viewing Wide Field-of-view Sensor (SeaWiFS) during extensive summer algae (cyanobacterial) blooms in July 1997 (Northern Baltic Proper), in August 1999 (Southern Baltic Proper). Both natural and man-made surface films affect the sea surface and thus are visible on satellite imagery [4,5,12].

Although we have selected two cases for this paper, we want to underline that the algorithms are applicable to other imagery and to other areas than the Baltic Sea, if there are current tracers visible and the images are taken within a certain time period. In another example, we used SAR data from the California coastal area to derive sea surface currents.

3. IMAGE ANALYSIS USING SPATIAL CONSTRAINTS

In earlier studies [12], we have already demonstrated the use of motion detection / motion measurement algorithms for the derivation of sea surface currents.

Regarding the algorithms used, we can distinguish between feature-based and Optical Flow methods. Whereas feature-based methods only measure the movement of given features, the Optical Flow methods estimate the motion for the complete image domain. Therefore, we will distinguish between the use of spatial constraints into the next two chapters, because both handle them in a different way.

3.1. Adding spatial constraints to feature-based methods

In [12] we have already shown that data from sensors working at different electromagnetic frequency bands (e.g.,
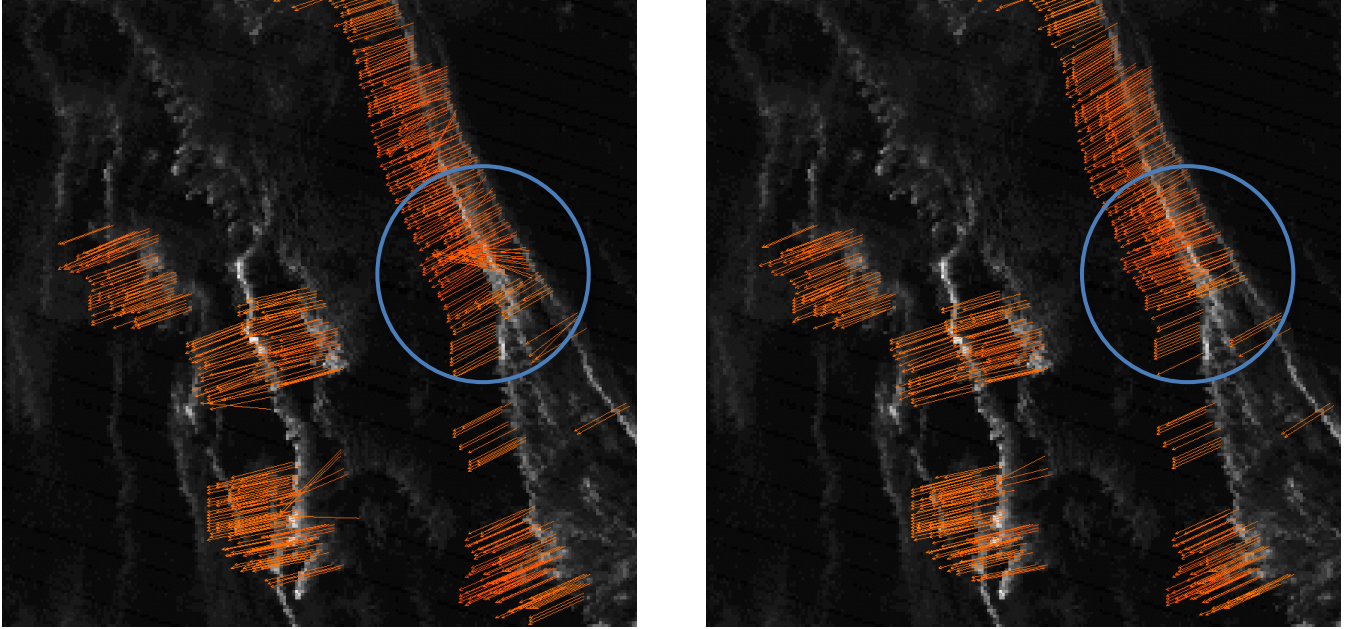
Fig. 1. The application of a relaxation algorithm on sea surface currents derived using a correlation approach on a Thematic Mapper (TM) (background image) and a Synthetic Aperture Radar (SAR) image. Left: The result of the normalized maximum cross correlation (MCC) feature-matching method. Right: The same result, but after the application of a relaxation algorithm. Motion vectors with a cross correlation lower than 0.60 are not displayed.

TM and SAR) can be used to apply high-speed feature-matching (cross-correlation) techniques for motion detection [7]. The drawback of these locally applied feature-matching algorithms is that they do not take into account the smoothness of motion within some spatial neighborhood. In order to overcome this drawback we have embedded a spatio-temporal constraint into the results of the feature-matching methods by means of applying relaxation techniques after the computation of sea surface currents based on feature matching [2, 11]. Note that the matching algorithm has to provide a set of (alternative) motion directions in order to apply a relaxation algorithm.

The application of this technique leads to a maximization of the 'global' (i.e., underlying) smoothness inside a given neighborhood. Therefore, alternative motion targets have to be estimated a priori. This approach is very different from general vector field smoothing operations (e.g., the replacement of each motion vector by the average motion vectors in some spatial neighborhood), since the relaxation techniques only selects alternative motion targets for each vector and does not introduce new (smoothed) vectors.

The first step of a relaxation algorithm is to find the neighbored motion vectors for each vector within a given radius. After that, the relaxation algorithm runs iteratively to optimize for a smooth flow inside a given neighborhood step by step. At each iteration step, the best fitting candidate from the list of all found candidates is determined and set to be the new valid vector for the next iteration. For the determination of the best fitting candidate, an "optimal

vector" by means of smoothness within the neighborhood is computed first. This is done by computing a mean vector inside the given neighborhood using Gaussian-weighted distances to the current vector.

After the application of the relaxation our results are also compared with the numerical model results of the sea surface currents provided by the German Federal and Maritime Agency (BSH) [6]. The vector field comparison is not a trivial task, because of the different spatio-temporal and (water) depth resolution of the derived and the model currents [10,14].

3.2. Spatial constraints in Optical Flow methods

In other cases, best results in computing sea surface currents are obtained through the calculation of the Optical Flow between subsequent images acquired by the same sensor (e.g. SeaWiFS) [12]. Optical Flow algorithms are implicitly based on the assumption that the motion is smooth within a certain spatial neighborhood [5]. Due to different smoothness assumptions and minimization strategies, several approaches exist.

In this paper, we will focus on the Lucas-Kanade algorithm [1,9]. It is based on constant motion assumption within a certain neighborhood:

$$\begin{bmatrix} v_x \\ v_y \end{bmatrix} = \begin{bmatrix} \sum I_{x_i}^2 & \sum I_{x_i} I_{y_i} \\ \sum I_{x_i} I_{y_i} & \sum I_{y_i}^2 \end{bmatrix}^{-1} \begin{bmatrix} -\sum I_{x_i} I_{t_i} \\ -\sum I_{y_i} I_{t_i} \end{bmatrix} \quad (1)$$
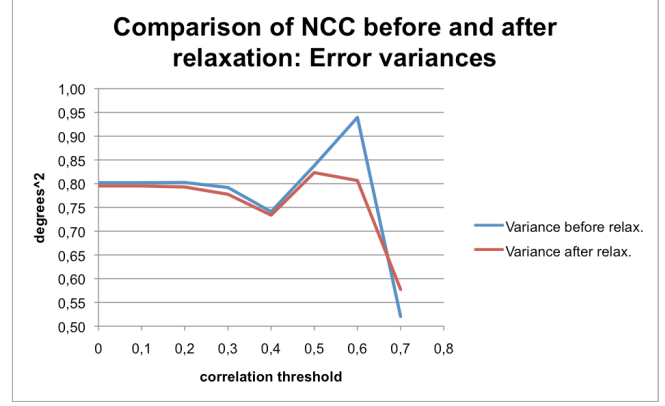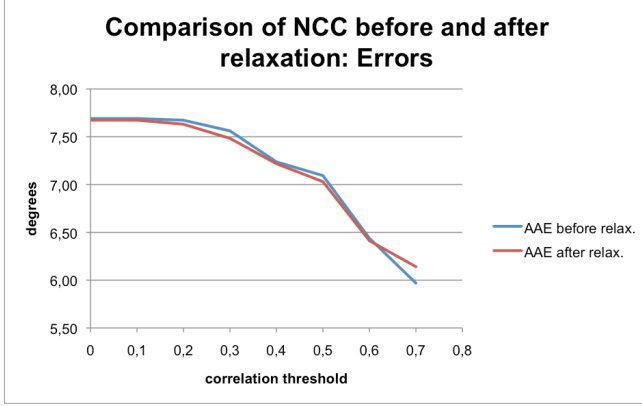
Fig. 2. The errors (left) and the error deviations (right) when comparing the NCC motion vector field to the BSH v2 model results, and when comparing the result of the relaxation to the same model results.

where v_x and v_y denote the motion in x- and y-direction, and I_x, I_y, and I_t are the partial derivatives of the images in x- and y-direction and time. The sums are running over a given neighborhood for each pixel.

Regarding the sums in Eq. 1, we recognize the uniform weighting of image information in the neighborhood. Especially, there is no weighting for favoring closer image information. To add the distance dependency, we transform the Lucas Kanade algorithm into a Structure Tensor approach, which changes the neighborhood smoothness constraint from a constant to a distance weighted Gaussian function. Thus, image information that is more distant from the current position will be less weighted:

$$\begin{bmatrix} v_x \\ v_y \end{bmatrix} = \begin{bmatrix} G\left(I_x^2, \sigma\right) & G\left(I_xI_y, \sigma\right) \\ G\left(I_xI_y, \sigma\right) & G\left(I_y^2, \sigma\right) \end{bmatrix}^{-1} \begin{bmatrix} -G\left(I_xI_t, \sigma\right) \\ -G\left(I_yI_t, \sigma\right) \end{bmatrix} \quad (2)$$

where $G(x, \sigma)$ denotes the Gaussian function. The *2×2* matrix that needs to be inverted is called the Structure Tensor at scale σ, which gives the approach its name. Note that this distance-weighted approach is also used for the determination of the "optimal vector" during the relaxation. Again, we compare the results of these two algorithms with the numerical model results provided by local agencies.

4. RESULTS

According to the different types of spatial constraints, we separate the results into two chapters for clarity. In the first chapter we will present the results of the relaxation algorithm, whereas in the second chapter, we show the differences between the Lucas Kanade and the Structure Tensor approach.

4.1. The influence of relaxation as post-processing step

As an example for this case, Fig. 1 shows sea surface currents (yellow arrows) derived using a pair of ERS SAR and Landsat TM images. Blue circles highlight regions of main improvement: in those areas calculation errors such as crossing vectors (arrows) in the left panel are corrected in the relaxed vector field in the right panel. Our results (left panel) represent the local smoothness much better, without reducing the correlation factor for each (local) motion.

Although the relaxation algorithm is only supposed to correct some outliers (see Fig. 1), we see that the enhancement of quality is visible even when comparing the whole vector field with the model data (see Fig. 2). The average angular error (compared to the model data) decreases for nearly all correlation classes, except for the motion vectors of highest correlation (see Fig. 2, left panel). The variances are also rapidly decreasing between a correlation threshold of 0.4 and 0.6, which mainly indicates, that the relaxation algorithm was able to decrease the variance of the motion vectors.

4.2. From Lucas Kanade to the Structure Tensor approach

To measure the influence of the different spatial constraints of both algorithms, we compute several sea surface current vector fields with different mask-sizes. Then we compared each computed vector field to the predicted currents of the BSH v3 model using the method proposed in [13]. Note that we have to choose appropriate values for the Gaussian standard deviation, in order to make the results comparable to the mask size of the Lucas Kanade algorithm.

The resulting average angular errors and their variances are plotted in Fig. 3. We see an advantage of the Structure Tensor method over the Lucas Kanade method in both the decreasing error and its variance. There seems to be some convergence in the errors for large mask-sizes. This may be caused by a "smoothing out" of nearly all image information.

However, due to small turbulent structures that are found by both algorithms but not predicted by the BSH v3 model, the overall errors and variances are much higher than for the feature matching case presented earlier.
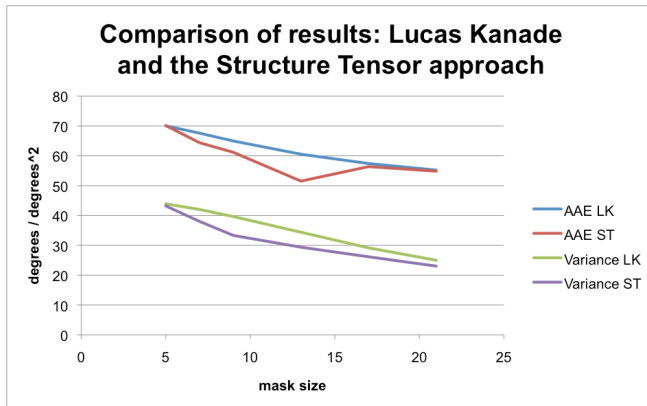
Fig. 3. Comparison of the average angular errors for derived currents using the Lucas Kanade (LK) and Structure Tensor (ST) approach when compared to model data of the BSH v3 model.

5. CONCLUSIONS

We demonstrated that the addition, or the change, of spatial constraints in the presented algorithms leads to promising results of the derivation of sea surface currents from satellite data. The use of relaxation techniques as a post-processing step after the derivation of currents using feature-matching methods seems to be very valuable, as these algorithms do not take any smoothness of motion into account. In addition, the relaxation approach does not smooth the vector field but tries to optimize using alterative directions (see Fig. 1).

The correct choice of smoothness is important for gradient-based Optical Flow algorithms. We have shown that the Structure Tensor approach leads to more reliable results than the Lucas Kanade method, when applied for the derivation of sea surface currents due to the different spatial relationship model of the Structure Tensor approach.

Our results clearly show that satellite images may be used to derive mesoscale sea surface currents, but also that special attention has to be paid to the very kind of algorithm used. We also note that sea surface features visible on the used satellite imagery must be present, in order to allow for successful surface current computation. Any kind (i.e., biogenic or anthropogenic) of sea surface films is well suited in this respect.

6. ACKNOWLEDGMENTS

7. REFERENCES

[1] Baker and Matthews, 2004, Lucas-Kanade 20 years on: A unifying framework. In International Journal of Computer Vision, 56(3):221–255, 2004.

[2] Chen, Lin, and Kung, 1996. A feature tracking algorithm using neighborhood relaxation with multi-candidate pre-screening. Image Processing, 1996. Proceedings., International Conference on, vol.1, no., pp.513-516 vol.2

[3] Gade, Alpers, Hühnerfuss, Masuko and Kobayashi, 1998a. The Imaging of Biogenic and Anthropogenic Surface Films by the Multi-frequency Multi-polarization SIR-C/X-SAR. J. Geophys. Res. (103), pp. 18851–18866.

[4] Gade, Rud, and Ishii, 1998b. Monitoring algae blooms in the Baltic Sea by using spaceborne optical and microwave sensors. Proceed. IGARSS '98. pp. 754–756.

[5] Horn and Schunck, 1981. Determining Optical Flow. Artificial Intelligence.

[6] Kleine, 1994. Das operationelle Model des BSH für Nordsee und Ostsee, Konzeption und Übersicht. Technical report, Bundesamt fur Seeschiffahrt und Hydrographie. Hamburg.

[7] Lewis, J. P., 1995. Fast Normalized Cross-Correlation. In Vision Interface, Canadian Image Processing and Pattern Recognition Society, pp. 120–123.

[8] Lucas and Kanade, 1981. An iterative image registration technique with an application to stereo vision. In Proceedings of the 7th International Conference on Artificial Intelligence, pages 674–679, August 1981.

[9] Mark, 2009. Entwicklung eines Werkzeuges zur Messung der Genauigkeit von Bewegungsfeldern der Meeresoberfläche. Diploma Thesis, Cognitive Systems Laboratory, Dept. Informatics, University of Hamburg

[10] Price, 1985. Relaxation Matching Techniques-A Comparison. Pattern Analysis and Machine Intelligence, IEEE Transactions on 1985, PAMI-7, 617-623.

[11] Rud and Gade, 2000. Using multi-sensor data for algae bloom monitoring. Proceed. IGARSS 2000., pp. 1714–1716 vol.4.

[12] Seppke, Gade, Dreschler-Fischer. 2009. Sea Surface Current Fields in the Baltic Sea Derived From Multi-Sensor Satellite Data. Proceed. ISPRS Workshop 2009: High-Resolution Earth Imaging for Geospatial Information

[13] Seppke, Gade, Dreschler-Fischer. Evaluation of High-Resolution Sea Surface Current Fields in the Baltic Sea Derived from Multi-Sensor Satellite Imagery, submitted to ESA Living Planet Symposium 2010